

Sci. **A3**, 681 (1963).

<sup>32</sup>For an authoritative review of the theory of dissociative electron attachment, see Ref. 4.

<sup>33</sup>D. Rapp and D. D. Briglia, *J. Chem. Phys.* **43**, 1480 (1965).

<sup>34</sup>Due to the low ion currents at  $\sim 10$  eV it was not possible to measure accurately the kinetic energies of the ions in this energy region by a retarding analysis similar to that performed on the  $\sim 6$ -eV peaks. The interesting

suggestion<sup>16</sup> that  $\text{NH}_2^-$  from the 10-V peak is formed in a highly excited state therefore remains a possibility.

<sup>35</sup>For these particular measurements the effect of thermal motion of the molecule prior to attachment upon the dissociating particles in ion retardation measurements [P. J. Chantry and G. J. Schulz, *Phys. Rev.* **156**, 134 (1967)] is approximately the same as the limits of error placed upon the determined dissociation energy ( $\sim 0.15$  eV).

## Optical Potential for Li-HBr Collisions at Low Energies \*

R. Marriott<sup>†</sup> and David A. Micha

*Department of Physics and Institute for Pure and Applied Physical Sciences, University of California, San Diego, La Jolla, California 92037*

(Received 9 December 1968)

A molecular optical potential has been used to reproduce the quenching of glory undulations in the total cross section of Li and HBr colliding at relative velocities  $10^5 \text{ cm/sec} \leq v \leq 3.10^5 \text{ cm/sec}$ . The experimental results over the whole velocity range are well fitted by a  $r^{-12}$  law for the imaginary part of the potential. Complex phase shifts, opacity function, and elastic angular distribution have been calculated with this potential. Comparison with calculations using a real potential shows rainbow and supernumerary rainbow maxima and an increase of intensities at large angles in both cases. The main effect of inelastic transitions is to decrease the scattering intensity at large center of mass angles.

### I. INTRODUCTION

We present in this contribution results on a molecular optical potential which reproduces the quenching (i. e., decrease in the amplitude) of glory undulations observed recently<sup>1</sup> in the total cross section of Li and HBr colliding in the range of relative velocities  $10^5 \text{ cm/sec} \leq v \leq 3.10^5 \text{ cm/sec}$ , or relative kinetic energies from 0.033 to 0.301 eV. Glory undulations were predicted<sup>2</sup> and measured<sup>3</sup> some time ago for atom-atom collisions and their origin is well understood. More recently, measurements made with crossed beams of atoms and molecules indicate a quenching of these glory undulations that can in general be attributed to excitation of vibration-rotation levels of the molecule and to reaction.<sup>4-7</sup>

### II. OPTICAL POTENTIAL FOR Li+HBr

In the case of Li+HBr at the relative kinetic energies investigated, excitation of vibrational levels is forbidden by energy conservation. Contribution of reactions in the region of impact pa-

rameters relevant to the glory effect is expected to be small.<sup>1,6</sup> The quenching may then be attributed to rotational excitation of HBr. This is interpreted here as equivalent to absorption of the scattering flux, and may be discussed in terms of optical (complex) molecular potentials.<sup>8</sup> Such a potential, taken as

$$U(r) = V(r) - iW(r) \quad (1)$$

was used to solve a system of two radial equations for the scattering function  $y(r)$ , with asymptotic form

$$y(r) \sim kr \{ j_l(kr) + t_l(k) [n_l(kr) + i j_l(kr)] \}, \quad (2)$$

$$t_l(k) = (2i)^{-1} [\exp(2i\eta_l) - 1], \quad (3)$$

$$\eta_l = \xi_l + i\zeta_l, \quad (4)$$

where  $r$  is the interparticle distance,  $k$  the relative wave number, and  $j_l$  and  $n_l$  first- and second-class spherical Bessel functions. The equations

were solved numerically<sup>9</sup> with initial conditions corresponding to a hard-core repulsion within the classically forbidden region near the origin. For the real and imaginary part of the potential, the following functions were used:

$$V(r) = \epsilon [(r_m/r)^{12} - 2(r_m/r)^6], \quad (5)$$

$$W(r) = c\epsilon(r_m/r)^{12}. \quad (6)$$

The values for the well depth  $\epsilon = 4.85 \times 10^{-14}$  erg and its radial position  $r_m = 3.97$  Å were those deduced from the experiment. The imaginary part was chosen so that the flux divergence is peaked at about the turning point region for scattering, and decreases at large  $r$  as an inverse power. This behavior as  $r$  increases is suggested by calculations on rotational excitation, which show that a large number of rotational quantum numbers contribute to the cross section,<sup>10</sup> and by *a priori* calculations of optical potentials.<sup>8</sup> They indicate that the excitations are spread over a region of interparticle distances beyond the turning point. The factor  $c$  was taken independent of  $k$  and  $l$ , and calculations of phase shifts carried out for several  $c$  values. The comparison with experimental results can be seen clearly in terms of the experimental and computed glory-undulation amplitudes  $\Delta Q_g(k)$  in the total cross section  $Q_{\text{tot}}(k)$ . The quantity  $\Delta Q_g(k)$  is given in the stationary phase approximation<sup>11,12</sup> by

$$\begin{aligned} \Delta Q_g(k) &= (4\pi/k) \text{Im} f_g(k, 0) \\ &= (4\pi/k^2) l_g \exp(-2\xi_{l_g}) \pi \\ &\quad \times \left[ \left( -\frac{\partial^2 \xi_{l_g}}{\partial l^2} \right) \right]_{l_g}^{-1} \sin(2\xi_{l_g} - 3\pi/4), \end{aligned} \quad (7)$$

where  $f_g(k, \theta)$  is the contribution to the scattering amplitude from angular momenta around the glory value  $l_g$ . From the calculation, it was found that the shape of  $\xi_l$  around  $l_g$  was, for our purpose, the same whether we used the full optical potential (OP) or only its real part (RP). It follows then that, indicating with  $k_e$  the wave numbers at the extrema for each potential,

$$\begin{aligned} \xi_{l_g}(\text{calc}) \\ = -\frac{1}{2} \ln |\Delta Q_g(k_e)_{\text{OP}} / \Delta Q_g(k_e)_{\text{RP}}|, \end{aligned} \quad (8)$$

which may be compared with the experimental value  $\xi_{l_g}(\text{exp})$ , obtained by replacing  $\Delta Q_g(k_e)_{\text{OP}}$  with  $\Delta Q_g(k_e)_{\text{exp}}$  in Eq. (8). Results of calculations

with  $c = 0.044$  are shown in Fig. 1, together with several experimental points. It is seen that this choice of  $c$  reproduces closely the experimental results over the whole velocity range.

Phase shifts were computed in this and other cases for  $l \leq L$ , with  $L$  such that  $\xi_L \gtrsim 0.200$  and  $\xi_L \gtrsim 0.001$ . For  $l > L$  Jeffrey-Born phase shifts  $\eta_l(\text{JB})$  from the  $r^{-6}$  part of  $U(r)$  were used, given by

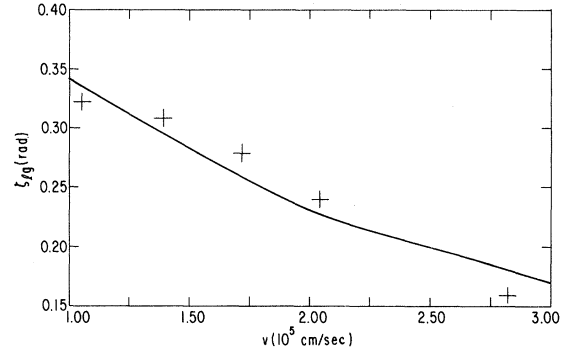


FIG. 1. Comparison of calculated  $\xi_{l_g}$  (solid lines) with values deduced from experiment (crosses), for  $c = 0.44$ , as functions of the relative velocity  $v$ .

$$\eta_l(\text{JB}) = \xi_l(\text{JB}) = a(l + \frac{1}{2})^{-5}, \quad (9)$$

with  $a = 3\pi\mu\epsilon r_m^6 k^4 / (8\hbar^2)$ . Phase shifts and the opacity function  $p_l = 1 - \exp(-4\xi_l)$  are given in Fig. 2 for  $v = 1.5 \times 10^5$  cm/sec and all  $l$  values. The opacity  $p_l$ , which measures the probability for nonelastic scattering, may be represented by

$$p_l = \frac{1}{2} p_c \{1 + \exp[(l - l_c)/d]\}, \quad (10)$$

where  $p_c$ ,  $l_c$ , and  $d$  are energy-dependent parameters. This functional form has been previously used in optical model calculations.<sup>13</sup> The optical potential method used here gives information on its energy dependence, that would otherwise be unknown.

The previous phase shifts have been used to predict the elastic angular distribution for Li + HBr. The elastic scattering amplitude was obtained from

$$f(\theta) = f_{<}(\theta) + f_{>}(\theta), \quad (11)$$

where  $f_{<}$  is the contribution from  $l \leq L$ ,

$$f_{<}(\theta) = k^{-1} \sum_{l=0}^L (2l+1) t_l \tilde{P}_l(\cos\theta), \quad (12)$$

$$\tilde{P}_l(\cos\theta) = 2[(2l+1)\pi \sin\theta]^{-1/2} \sin[(l + \frac{1}{2})\theta + \pi/4], \quad (13)$$

for  $\sin\theta \geq l^{-1}$ . The contribution  $f_{>}(\theta)$  from  $l > L$  was calculated using Eq. (9), transforming the

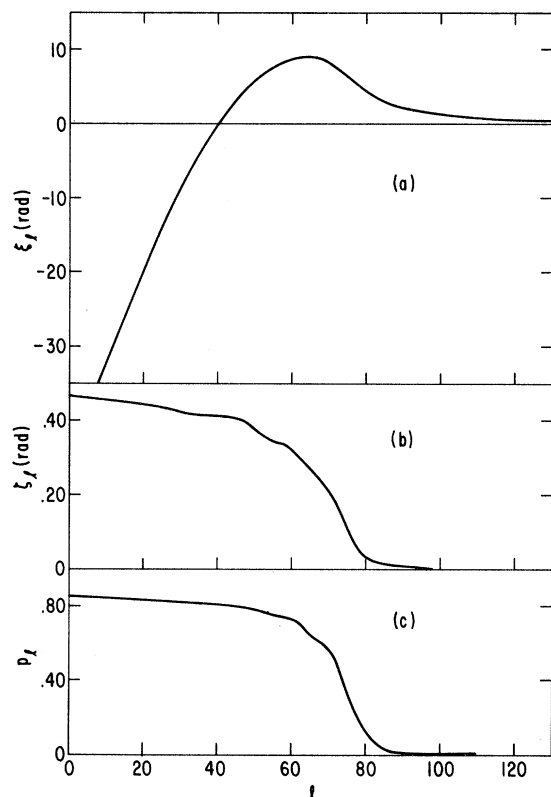


FIG. 2. (a) Real phase shifts, (b) imaginary phase shifts, and (c) opacity function at  $v = 1.5 \times 10^4$  cm/sec and for  $c = 0.44$  as functions of the orbital quantum number  $l$ .

sum over  $l$  into an integral and keeping only the lowest order in  $L^{-1}$ , which gives

$$f_{>}(\theta) = k^{-1} 4aL^{-4.5} (1 + iaL^{-5}) \times \cos(L\theta + \pi/4) / (2\pi\theta \sin\theta)^{1/2}. \quad (14)$$

The elastic angular distribution  $I_{el}(\theta) = |f(\theta)|^2$  was computed at intervals of one degree. Figure 3 shows  $I_{el}(\theta)$  for  $V(r)$  and also for  $U(r)$ . Rainbow and supernumerary rainbow maxima at small angles and a slight increase of intensities at large angles are noticeable in both curves. Comparing Fig. 3(a) and 3(b) it is seen that the main effect of inelastic transitions is to decrease the scattering intensity at large center of mass angles.

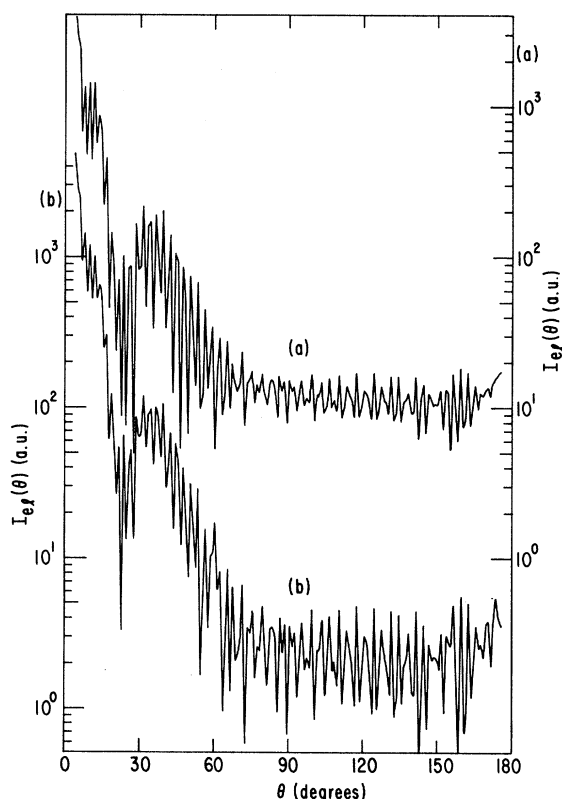


FIG. 3. (a) Differential cross section for real potential (scale at right) and (b) for optical potential (scale at left) versus center-of-mass scattering angle  $\theta$ .

### III. CONCLUSIONS

Semiphenomenological potentials of the type reported here should be useful in the interpretation of the rapidly increasing amount of experimental information on molecular-collision cross sections. They provide an alternative way of generalizing the intermolecular potentials currently used that might be useful to explain finer details of the thermodynamical and transport properties of liquids and gases and of chemical rate processes.

### ACKNOWLEDGMENTS

We thank R. K. B. Helbing and E. W. Rothe for communicating to us their experimental results before publication.

\*This research was supported by the Advanced Research Projects Agency of the Department of Defense and was monitored by the U. S. Army Research Office, Durham under Contract DA-31-124-ARO-D-257.

†Present address: Research Institute for Engineering

Sciences, College of Engineering, Wayne State University, Detroit, Michigan 48202.

<sup>1</sup>R. K. B. Helbing and E. W. Rothe, J. Chem. Phys. **48**, 3945 (1968).

<sup>2</sup>R. B. Bernstein, J. Chem. Phys. **34**, 361 (1961).

- <sup>3</sup>E. W. Rothe, P. K. Rol, S. M. Trujillo, and R. H. Neynaber, *Phys. Rev.* **128**, 659 (1962).
- <sup>4</sup>E. A. Gislason and G. H. Kwei, *J. Chem. Phys.* **46**, 2838 (1967).
- <sup>5</sup>H. L. Kramer and P. R. LeBreton, *J. Chem. Phys.* **47**, 3367 (1967).
- <sup>6</sup>R. E. Olson and R. B. Bernstein, *J. Chem. Phys.* **49**, 162 (1968).
- <sup>7</sup>R. T. Cross, Jr., *J. Chem. Phys.* **49**, 1976 (1968).
- <sup>8</sup>D. A. Micha, *Bull. Am. Phys. Soc.* **13**, 394 (1968); *J. Chem. Phys.* (to be published, 1969).
- <sup>9</sup>R. Marriott, *Proc. Phys. Soc. (London)* **72**, 121 (1958), Appendix.
- <sup>10</sup>A. C. Allison and A. Dalgarno, *Proc. Phys. Soc. (London)* **90**, 609 (1967), show the contribution of individual partial waves to rotational excitation cross sections.
- <sup>11</sup>R. B. Bernstein, *Advances in Chemical Physics*, edited by J. Ross (Interscience Publishers, New York, 1966) Vol. X, Chap. 3.
- <sup>12</sup>C. Nyland and J. Ross, *J. Chem. Phys.* **49**, 843 (1968).
- <sup>13</sup>R. B. Bernstein and R. D. Levine, *J. Chem. Phys.* **49**, 3872 (1968).

## Threshold Behavior of the Cross Section for Ionization of He and Ar by Mono-Energetic Electrons\*

P. Marchand, C. Paquet, and P. Marmet

*Centre de Recherches Sur Les Atomes et Les Molécules, Laval University, Quebec, Canada*

(Received 26 August 1968; revised manuscript received 16 December 1968)

A new apparatus using crossed-beam techniques with a cylindrical electrostatic electron velocity selector for the study of ionization probability curves of gases is described. Results for He<sup>+</sup> and Ar<sup>+</sup> in the first eV above the ionization threshold are given. New computer techniques determine structure and near-threshold behavior. A simple power law yields a good representation of the experimental results for each ion state, with a different power in each case. For He a power law with power 1.16 is found. The results for Ar may be represented by two power laws with powers 1.3 and 1.34, respectively, joining at the energy of the <sup>2</sup>P<sub>1/2</sub> level of Ar<sup>+</sup>.

### INTRODUCTION

The study of ionization by electron impact near the ionization threshold is of considerable interest for the determination of electron-neutral interaction laws, and has been the object of a considerable number of experimental and theoretical works. The experimental work, however, has not yet always yielded the results hoped for, as witnessed by the lack of agreement between the results from different laboratories and by the lack of reproducibility of results in general.

For instance, there has been considerable difficulty in the past in obtaining sufficiently large currents of fairly monoenergetic electrons at energies from 10 to 25 eV. Although the introduction of the retarding-potential-difference (RPD) method<sup>1</sup> and of spherical<sup>2</sup> and cylindrical<sup>3</sup> electrostatic electron velocity selectors has permitted narrower energy spreads, the limited electron

energy resolution is still somewhat of a problem.

Another difficulty<sup>4</sup> is that in a 1-cm<sup>3</sup> Nier-type ionization chamber, at pressures as low as 10<sup>-5</sup> Torr, if there is a monolayer of gas on the surface, then there are 10<sup>4</sup>–10<sup>5</sup> times more molecules on the walls than in the volume enclosed. The ionization potential of molecules on the wall may be slightly different from that for corresponding free molecules, and thus change the shape of ionization probability curves.

Recent measurements of surface phenomena<sup>4-6</sup> reveal another source of experimental errors. They indicate, for instance, that it is quite difficult to obtain the field-free or at least constant low-field region necessary for accurate measurements of ionization cross sections; and a field in this region, caused by such surface phenomena, can greatly influence the ion collection efficiency as well as broaden the electron energy spread.

Many other sources of systematic errors due to